

Vanishing Higgs potential at the Planck scale in a singlet extension of the standard model

Naoyuki Haba,¹ Hiroyuki Ishida,¹ Kunio Kaneta,² and Ryo Takahashi¹

¹*Graduate School of Science and Engineering, Shimane University,
Matsue, Shimane 690-8504, Japan*

²*ICRR, University of Tokyo, Kashiwa, Chiba 277-8582, Japan*

Abstract

We discuss the realization of a vanishing effective Higgs potential at the Planck scale, which is required by the multiple-point criticality principle (MPCP), in the standard model with singlet scalar dark matter and a right-handed neutrino. We find the scalar dark matter and the right-handed neutrino play crucial roles for realization of the MPCP, where a neutrino Yukawa becomes effective above the Majorana mass of the right-handed neutrino. Once the top mass is fixed, the MPCP at the (reduced) Planck scale and the suitable dark matter relic abundance determine the dark matter mass, m_S , and the Majorana mass of the right-handed neutrino, M_R , as $8.5 (8.0) \times 10^2 \text{ GeV} \leq m_S \leq 1.4 (1.2) \times 10^3 \text{ GeV}$ and $6.3 (5.5) \times 10^{13} \text{ GeV} \leq M_R \leq 1.6 (1.2) \times 10^{14} \text{ GeV}$ within current experimental values of the Higgs and top masses. This scenario is consistent with current dark matter direct search experiments, and will be checked by future experiments such as LUX with further exposure and/or the XENON1T.

1 Introduction

The Higgs particle was discovered at the LHC experiment [1, 2], but one finds no evidence to support the existence of physics beyond the standard model (SM) so far. Thus, the question “How large is new physics scale?” is important for the SM and new physics. One simple answer is that the SM is valid up to the Planck scale; i.e., there is no new physics between the electroweak (EW) and the Planck scales. In that case, the current experimental values of the Higgs and top masses might imply a vanishing effective Higgs potential at the Planck scale. In fact, there are intriguing researches about this possibility. For instance, Ref. [3] proposed the multiple-point criticality principle (MPCP). This principle means that there are two degenerate vacua in the SM Higgs potential, $V(v) = V(M_{\text{pl}}) = 0$ with $V'(v) = V'(M_{\text{pl}}) = 0$, where V is the effective Higgs potential, v is the vacuum expectation value (VEV) of the Higgs, and M_{pl} is the Planck scale. One is at the EW scale where we live, and another is at the Planck scale, which can be realized by the Planck-scale boundary conditions (BCs) of the vanishing Higgs self-coupling [$\lambda(M_{\text{pl}}) = 0$] and its β function [$\beta_\lambda(M_{\text{pl}}) = 0$]. As a result, Ref. [3] pointed out that the principle predicts a 135 ± 9 GeV Higgs mass and a 173 ± 5 GeV top mass, which are close to the experimental values but not the current center values. Furthermore, an asymptotic safety scenario of gravity [4] predicted 126 GeV Higgs mass with a few GeV uncertainty, and this scenario also pointed out $\lambda(M_{\text{pl}}) \simeq 0$ and $\beta_\lambda(M_{\text{pl}}) \simeq 0$ (see also Refs. [5]-[14] for more recent analyses). In this paper, we discuss the realization of a vanishing effective Higgs potential at the Planck scale, which is required by the MPCP, in the SM with singlet scalar dark matter (DM) and a right-handed neutrino.

An important motivation of the gauge singlet extension of the SM is to explain DM and the tiny active neutrino mass. In this extension, the scalar particle can be DM when it has odd parity under an additional Z_2 symmetry [15] (see also Refs. [16]-[26]). The right-handed Majorana neutrino can generate the tiny active neutrino mass via the type-I seesaw mechanism. Once the scalar (right-handed neutrino) is added to the SM, an additional positive (negative) contribution appears in β_λ .¹ In addition, since it is difficult to reproduce the 126 GeV Higgs mass and the 173.34 ± 0.76 GeV top pole mass [33] at the same time under the MPCP at the Planck scale in the SM, it is intriguing to study whether the principle can be realized with the center values of the Higgs and top masses in the singlet extension of the SM, or not.

In this paper, we discuss the realization of the vanishing effective Higgs potential at the Planck scale, which is required by the MPCP, in the SM with singlet scalar DM and the right-handed neutrino. Intriguingly, both the scalar DM and the right-handed neutrino are necessary to realize the MPCP which predicts the DM mass m_S and the Majorana mass of the right-handed neutrino M_R : $8.5 (8.0) \times 10^2 \text{ GeV} \leq m_S \leq 1.4 (1.2) \times 10^3 \text{ GeV}$ and $6.3 (5.5) \times 10^{13} \text{ GeV} \leq M_R \leq 1.6 (1.2) \times 10^{14} \text{ GeV}$ within current experimental values of the Higgs and top masses.

¹See also Refs. [18, 23, 24] for researches of the vacuum stability and the coupling perturbativity in the SM with scalar DM, and Refs. [27, 28, 29, 30] for explaining the recent BICEP2 result [31] in the framework of the Higgs inflation [32] with gauge singlet fields.

2 Singlets extension of the SM

The relevant Lagrangians of the singlet extension of the SM are given by

$$\mathcal{L} = \mathcal{L}_{\text{SM}} + \mathcal{L}_{\text{singlets}}, \quad (1)$$

$$\mathcal{L}_{\text{SM}} \supset -\lambda \left(|H|^2 - \frac{v^2}{2} \right)^2, \quad (2)$$

$$\mathcal{L}_{\text{singlets}} = -\frac{\bar{m}_S^2}{2} S^2 - \frac{k}{2} |H|^2 S^2 - \frac{\lambda_S}{4!} S^4 - \left(\frac{M_R}{2} \overline{N^c} N + y_N \overline{L} \tilde{H} N + c.c. \right) + (\text{kinetic term}), \quad (3)$$

where the SM Lagrangian including the effective Higgs potential is given by \mathcal{L}_{SM} , and H is the Higgs doublet ($\tilde{H} \equiv -i\sigma_2 H^*$), S is a gauge singlet real scalar field, L is the left-handed lepton doublet of the SM, N is the right-handed neutrino, y_N is the neutrino Yukawa coupling, and M_R is the Majorana mass of the right-handed neutrino. In the model, since only the singlet real scalar is assumed to have odd parity under an additional Z_2 symmetry, it can be DM with suitable mass and couplings. The DM mass is given by $m_S = \sqrt{\bar{m}_S^2 + kv^2/2}$. The right-handed neutrino generates the small active neutrino mass through the type-I seesaw mechanism.

We utilize the renormalization group equations (RGEs) at two-loop level in this model, which were first given in Ref. [30]. Here, we mention the features of RGE runnings of the scalar quartic couplings at the two-loop level:

1. Since the β function of k is proportional to k itself, an evolution of k is tiny when $k(M_Z)$ is close to zero. Note that $k(M_Z) \rightarrow 0$ is the SM limit.
2. $\lambda(\mu)$ becomes negative within $\mathcal{O}(10^{10})$ GeV $\lesssim \mu \leq M_{\text{pl}}$ when the experimental center values of the Higgs and top masses are taken; this is known as the vacuum instability or meta-stability in the SM. This is induced from the dominant negative contribution of the top Yukawa coupling, $-6y^4$. NNLO computations [7] indicate that $\lambda(\mu)$ can be positive within $M_Z \leq \mu \leq M_{\text{pl}}$ for the Higgs mass as $127 \text{ GeV} \leq m_h \leq 130 \text{ GeV}$ with a top mass of $M_t = 173.1 \pm 0.6 \text{ GeV}$ or $171.3 \text{ GeV} \leq M_t \leq 171.7 \text{ GeV}$, with $m_h = 126 \text{ GeV}$ (see also Ref. [14]).
3. The RGE evolution of λ can be raised by the additional positive term $+k^2/2$ in the β function of λ . There is also a negative contribution $-2y_N^4$ to the β function of λ from the neutrino Yukawa coupling, which pushes down the RGE evolution of λ . We will investigate whether the MPCP can be realized by considering these two contributions in the model, or not.

3 Multiple point criticality principle in singlets extension of the SM

The MPCP requires that there exist two degenerate vacua in the effective Higgs potential. One is at the EW scale where we live and another is at the Planck scale. This principle is described as $V(v) = V(M_{\text{pl}}) = 0$. In terms of λ and β_λ , this principle is written as

$$\lambda(M_{\text{pl}}) = 0, \quad \beta_\lambda(M_{\text{pl}}) = 0, \quad (4)$$

which is obtained from the stationary condition, $V'(H) = 0$. The conditions cannot be realized in the SM within the current experimental ranges of top and Higgs masses; i.e., the MPCP in the SM requires a lighter top mass and/or a heavier Higgs mass [3]. Thus, we need to consider an extension of the SM anyhow.

We investigate a realization of Eq. (4) in the singlet extension of the SM by solving the two-loop-level RGEs. The scalar DM (neutrino Yukawa) coupling lifts up (pushes down) the running of λ . Thanks to these two contributions in this extension, the positive contribution from the scalar to β_λ can avoid the metastable vacuum of the SM with the current experimental values of the top and the Higgs masses. The scalar contribution becomes dominant in β_λ at the Planck scale, which can realize $\lambda(M_{\text{pl}}) > 0$ and $\beta_\lambda(M_{\text{pl}}) > 0$. And a negative contribution from the neutrino Yukawa coupling to β_λ above the Majorana mass scale can successfully achieve $\lambda(M_{\text{pl}}) = 0$ and $\beta_\lambda(M_{\text{pl}}) = 0$. This is the essence of the realization of the MPCP in this singlet extension of the SM, and the realization is nontrivial. For the RGEs, decoupling effects of the scalar and the right-handed neutrino should be taken into account below their mass scales by taking away their relevant couplings from the corresponding β functions. In particular, it is very important that the neutrino Yukawa becomes effective above the Majorana mass of the right-handed neutrino. For the neutrino sector, the active neutrino mass is induced from the seesaw mechanism [$m_\nu = y_N^2 v^2 / (2M_R)$] and is taken as $m_\nu = 0.1$ eV. With these relations, the value of $y_N(M_Z)$ is given by $y_N(M_Z) = \sqrt{2m_\nu M_R} / v$. This is an example in which one active neutrino mass is obtained. Two other neutrino masses can also be effective in the RGE analyses, but here we assume that other neutrino Yukawa couplings are small enough to be neglected in the analyses.

Our results are summarized in Fig. 1, where the conditions of $\lambda = 0$ and $\beta_\lambda = 0$ are depicted by blue and orange curves, respectively. We analyze the realization of the MPCP at both the Planck M_{pl} and the reduced Planck scales \tilde{M}_{pl} , which are shown by the dashed and solid curves in all figures, respectively. In the regions above (below) the blue and orange solid curves, $\lambda(M_{\text{pl}}) > 0$ and $\beta_\lambda(M_{\text{pl}}) > 0$ [$\lambda(M_{\text{pl}}) < 0$ and $\beta_\lambda(M_{\text{pl}}) < 0$], respectively. These correspondences are the same for the case of the reduced Planck scale. Figures 1 (a)-1 (d) are the cases of $(M_t [\text{GeV}], \lambda_S(M_Z)) = (172.6, 10^{-3}), (174.1, 10^{-3}), (172.6, 0.5), \text{ and } (174.1, 0.5)$, respectively, with $\Omega_S h^2 = \Omega_{\text{DM}} h^2 = 0.12$ [34], where Ω_S is the density parameter of S , Ω_{DM} is for DM, and h is the Hubble constant. Since S is DM in the model, the value of $k(M_Z)$ is determined by m_S and Ω_S . We utilize micrOMEGAs [35] to estimate the relic abundance of S , and we take the

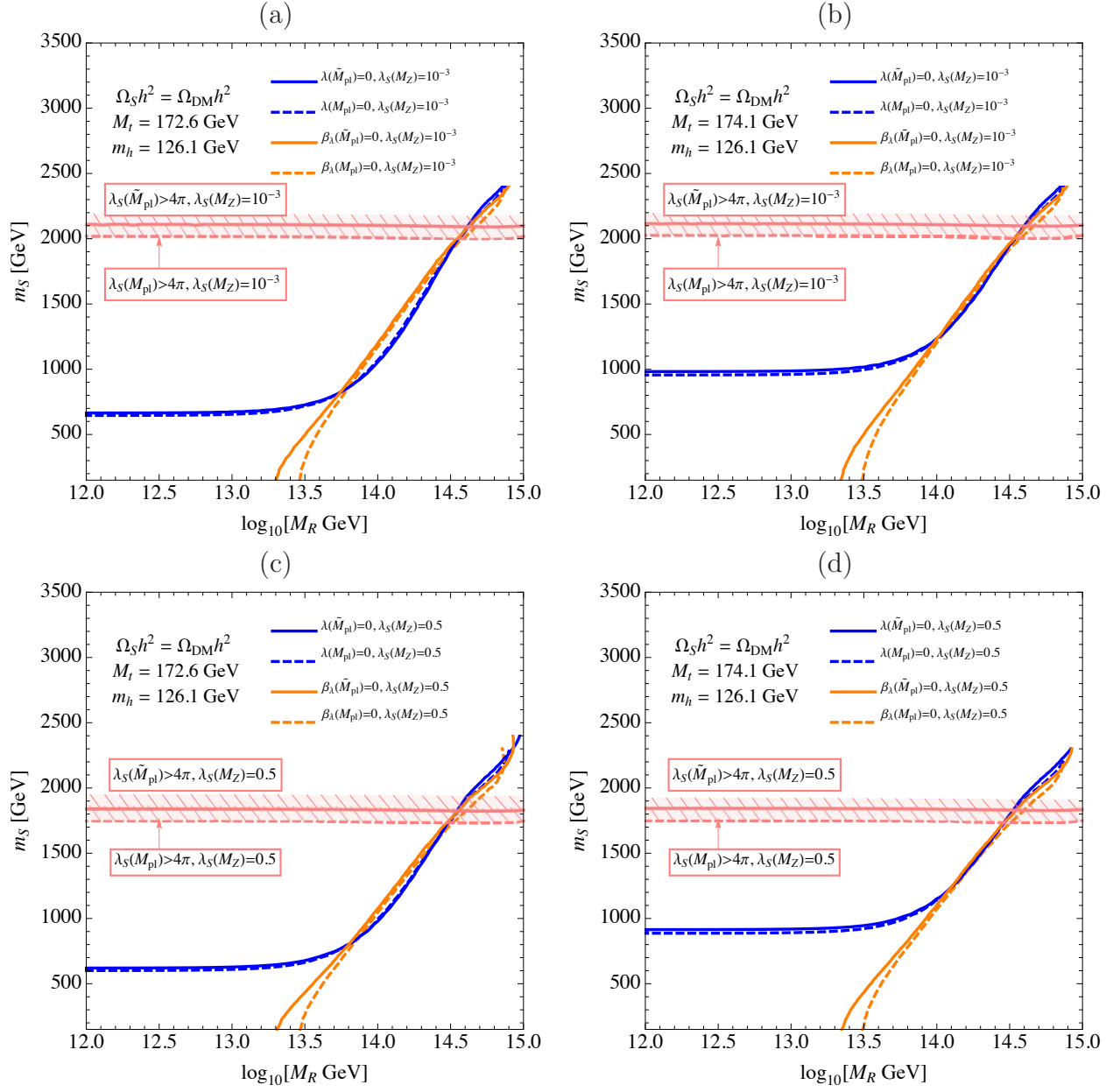


Figure 1: Numerical results for the realization of the MPCP [$\lambda = 0$ (blue curve) and $\beta_\lambda = 0$ (orange curve)]. The contours for the two conditions at the Planck M_{pl} and the reduced Planck \tilde{M}_{pl} scales are shown by the dashed and solid curves in all figures, respectively. Figures (a), (b), (c), and (d) correspond to the cases of $(M_t [\text{GeV}], \lambda_S(M_Z)) = (172.6, 10^{-3})$, $(174.1, 10^{-3})$, $(172.6, 0.5)$, and $(174.1, 0.5)$, respectively.

Higgs mass as 126.1 GeV in the calculation.² In the region above the pink dashed and solid lines, self-coupling λ_S exceeds 4π at the Planck and reduced Planck scales, respectively, while perturbative calculation is valid in the parameter space below the pink lines. At an intersection point of the blue and orange solid (dashed) curves below the horizontal pink solid (dashed) line, the MPCP can be satisfied within the experimentally allowed region of the Higgs, top, and DM masses with suitable scalar quartic couplings up to the (reduced) Planck scale. One can really see that there are some intersection points in Fig. 1. We mention parameter dependences for the realization of the MPCP as follows:

1. When M_R is relatively light, as $M_R < \mathcal{O}(10^{13})$ GeV, the contribution from the neutrino Yukawa coupling to β_λ is negligible. Thus, once M_t is fixed, $\lambda = 0$ is realized by taking suitable value for only m_S . This is shown by flat regions of blue curves in the figures. In this region, $\beta_\lambda(M_{\text{pl}})$ is always positive. A similar case, i.e. the decoupling limit of the right-handed neutrino $y_N \rightarrow 0$, was discussed in Ref. [24], and our analysis is consistent with the results of Ref. [24].
2. When M_R becomes large, we can successfully achieve $\beta_\lambda(M_{\text{pl}}) = 0$ with $\lambda(M_{\text{pl}}) = 0$. The correlation between m_S and M_R is seen in the slanting regions of the blue curves. One can see that a larger value of M_R is required to balance with the large scalar contribution.
3. Regarding the coupling perturbativity of $\lambda_S(M_{\text{pl}})$, it strongly depends on values of $k(M_Z)$ and $\lambda_S(M_Z)$ but not on M_R , because the neutrino Yukawa does not contribute to β_{λ_S} at the one-loop level. Thus, when one takes a larger $\lambda_S(M_Z)$, the bound of the coupling perturbativity of $\lambda_S(M_{\text{pl}})$ becomes severe for m_S .
4. For heavier M_t , the MPCP can be realized in heavier m_S , or equivalent to larger $k(M_Z)$ [compare Figs. 1(a) and 1(b), or Figs. 1(c) and 1(d)]. This is because the dominant negative contribution from the top Yukawa coupling in β_λ should be canceled by the positive contribution from k .
5. For larger $\lambda_S(M_Z)$, the MPCP is satisfied in lighter m_S [compare Fig. 1(a) and 1(c), or Figs. 1(b) and 1(d)]. Since λ_S coupling gives a positive contribution to the β function of k , k grows more rapidly for larger $\lambda_S(M_Z)$. As a result, smaller $k(M_Z)$ (or m_S) is favored for canceling the negative contribution from the top Yukawa coupling in a larger $\lambda_S(M_Z)$ case.

Next, Fig. 2 shows the positions of the intersection points in the $[M_R, M_t(\text{or } m_S)]$ plane for the $\lambda_S(M_Z) = 10^{-3}$ case.³ The solid and dashed curves indicate the MPCP solutions at \tilde{M}_{pl} and M_{pl} ,

²We also take the strong coupling as $\alpha_s = 0.1184$. For the matching terms of y_t and λ at the top pole mass scale, we take two-loop results, shown in e.g. Refs. [5, 7].

³One might also find another intersection point around $m_S \sim 2.0 \times 10^3$ GeV in each figure $[(m_S [\text{GeV}], M_R [\text{GeV}]) = (1.9 \times 10^3, 3.0 \times 10^{14}), (1.8 \times 10^3, 2.6 \times 10^{14}), (1.6 \times 10^3, 2.5 \times 10^{14}), \text{ and } (1.4 \times 10^3, 1.7 \times 10^{14})$ in Figs. 1(a), 1(b), 1(c), and 1(d), respectively]. Since these points are close to the

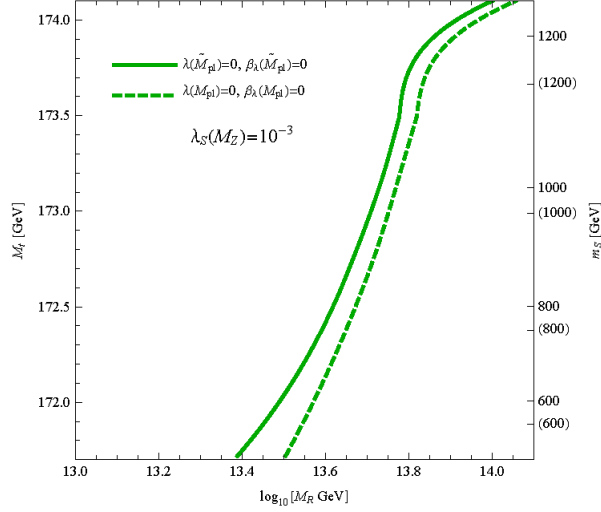


Figure 2: The positions of the intersection points in the $[M_R, M_t(\text{or } m_S)]$ plane for the $\lambda_S(M_Z) = 10^{-3}$ case. The solid and dashed curves indicate the MPCP solutions at M_{pl} and M_{pl} , respectively. The values in the parentheses on the m_S axis correspond to values in the case of the MPCP at the Planck scale while the m_S values without parentheses are for the case of MPCP at the reduced Planck scale.

respectively. We can show that m_S and M_R have one-to-one correspondence (m_S and M_t also have one to one correspondence). When one takes larger M_t , larger m_S and M_R are required to achieve $\lambda = 0$ and $\beta_\lambda = 0$ at the same time. To summarize, there are seven independent parameters; i.e., five coupling constants (λ , k , λ_S , y , and y_N) and two mass scales of the singlets (m_S and M_R), in the scalar and Yukawa sectors of the model, in which λ is determined by m_h . The suitable DM relic abundance relates k with m_S and the seesaw mechanism relates y_N with M_R . Thus, there are four independent parameters (λ_S , y , m_S , and M_R). When the top mass and λ_S are fixed, the two conditions of the MPCP ($\lambda = 0$ and $\beta_\lambda = 0$) uniquely determine m_S and M_R .⁴

As our result, we find that the MPCP at the (reduced) Planck scale predicts the following mass regions:

$$8.5 (8.0) \times 10^2 \text{ GeV} \leq m_S \leq 1.4 (1.2) \times 10^3 \text{ GeV}, \quad (5)$$

$$6.3 (5.5) \times 10^{13} \text{ GeV} \leq M_R \leq 1.6 (1.2) \times 10^{14} \text{ GeV}, \quad (6)$$

within $M_t = (172.6-174.1) \text{ GeV}$ and $10^{-3} \leq \lambda_S(M_Z) \leq 0.5$. They are obtained by maximal and minimal values of m_S and M_R on the intersection points of the two contours of the $\lambda = 0$ and

lines of the coupling perturbativity bound on λ_S , we do not consider these solutions around $m_S \sim 2.0 \times 10^3 \text{ GeV}$ in this paper anymore. But this could also be the solution for the MPCP.

⁴By extending the model, m_S and M_R could be induced dynamically from a dimensional transmutation, which could have a conformal or shift symmetry in the framework of conformal gravity as a UV theory.

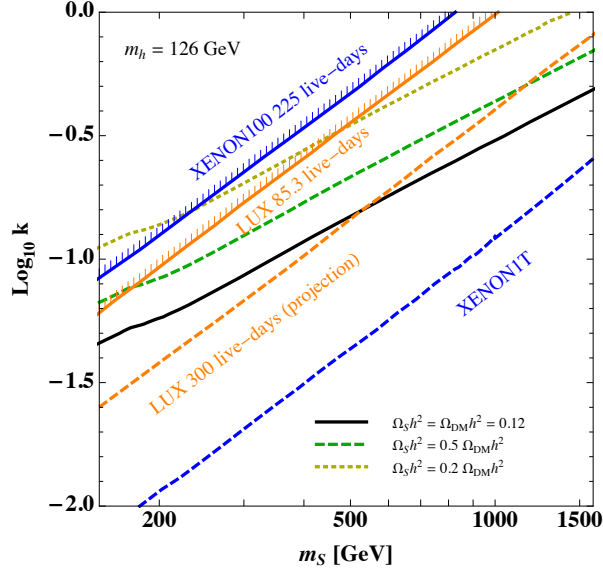


Figure 3: The current experimental bounds on m_S and k (XENON100 225 live-days (blue solid line) and LUX 85.3 live-days (orange solid line)), and the future detectability by the LUX 300 day projection (orange dashed line) and the XENON1T (blue dashed line) [36, 37]. The black solid curve indicates the contour of $\Omega_S h^2 = \Omega_{\text{DM}} h^2 = 0.12$. (The green and yellow dashed curves correspond to $\Omega_S h^2 = 0.5 \Omega_{\text{DM}} h^2$ and $0.2 \Omega_{\text{DM}} h^2$, respectively.)

$\beta_\lambda = 0$ lines which are located at $(m_S [\text{GeV}], M_R [\text{GeV}]) = (8.6 (8.2) \times 10^2, 6.3 (5.5) \times 10^{13})$, $(1.3 (1.2) \times 10^3, 1.1 (1.0) \times 10^{14})$, $(8.5 (8.0) \times 10^2, 7.4 (6.3) \times 10^{13})$, and $(1.4 (1.2) \times 10^3, 1.6 (1.2) \times 10^{14})$ for the case of the MPCP at the (reduced) Planck scale shown in Figs. 1(a), 1(b), 1(c), and 1(d), respectively.⁵

Finally, we draw Fig. 3, which shows the current experimental bounds on m_S and k [XENON100 225, live-days (blue solid line) and LUX, 85.3 live-days (orange solid line)] and the future detectability by the LUX (orange dashed line) and the XENON1T (blue dashed line) experiments [36, 37]. The black solid curve indicates the contour of $\Omega_S h^2 = \Omega_{\text{DM}} h^2 = 0.12$. One can find that the DM mass region in Eq. (5) for the realization of the MPCP can be consistent with the current DM direct detection experiments, and it will be checked by future DM direct searches, e.g., the future XENON1T experiment.

4 Summary and discussions

We have discussed the realization of the vanishing effective Higgs potential at the Planck scale, which is required by the MPCP, in the SM with the singlet scalar DM and the right-handed

⁵There are also intersection points around $m_S \sim 2.0 \times 10^3$ GeV in the reduced Planck case as $(m_S [\text{GeV}], M_R [\text{GeV}]) = (2.1 \times 10^3, 3.9 \times 10^{14})$, $(2.0 \times 10^3, 3.5 \times 10^{14})$, $(1.8 \times 10^3, 3.3 \times 10^{14})$, and $(1.7 \times 10^3, 2.8 \times 10^{14})$ in Figs. 1(a), 1(b), 1(c), and 1(d), respectively.

neutrino. We have found that the scalar DM and the right-handed neutrino play crucial roles for realization of the MPCP, where the neutrino Yukawa becomes effective above the Majorana mass of the right-handed neutrino. Once the top mass is fixed, the MPCP at the (reduced) Planck scale and the suitable DM relic abundance determine the DM mass and Majorana mass of the right-handed neutrino as $8.5 (8.0) \times 10^2 \text{ GeV} \leq m_S \leq 1.4 (1.2) \times 10^3 \text{ GeV}$ and $6.3 (5.5) \times 10^{13} \text{ GeV} \leq M_R \leq 1.6 (1.2) \times 10^{14} \text{ GeV}$ within the current experimental values of the Higgs and top masses. The m_S region is allowed by the current experimental results of the DM direct searches. Moreover, it is of importance that this scenario is testable by the future direct search experiments such as the LUX with further exposure and/or the XENON1T.

Finally, we also show other solutions of the MPCP as examples of different shares of Ω_S for Ω_{DM} ; i.e., $\Omega_S/\Omega_{\text{DM}} = 0.5$, shown in Figs. 4(a)-4(d), and 0.2 in Figs. 4(e)-4(h). The meanings of the lines and colors are the same as in Fig. 1. One can see that the MPCP can be realized in a lighter m_S region compared to the $\Omega_S/\Omega_{\text{DM}} = 1$ case. At the same time, the bound from the coupling perturbativity of λ_S on m_S becomes more severe when the value of $\Omega_S/\Omega_{\text{DM}}$ becomes smaller than unity (see Figs. 1 and 4). This is because a smaller Ω_S needs a larger value of $k(M_Z)$ for the same DM mass [e.g., see the green ($\Omega_S/\Omega_{\text{DM}} = 0.5$) and the yellow ($\Omega_S/\Omega_{\text{DM}} = 0.2$) dashed curves in Fig. 3]. Thus, a lighter m_S gives a solution for the MPCP, and a heavier m_S region is constrained by the coupling perturbativity of λ_S in a smaller $\Omega_S/\Omega_{\text{DM}}$ case. We also show excluded (shaded) regions of $m_S < 480 \text{ GeV}$ by the LUX 85.3 live-day WIMP search [36] in Figs. 4(e)-4(h). Regarding an experimental bound on DM, although there are intersection points around $m_S \sim 400 \text{ GeV}$ in the case of $\Omega_S/\Omega_{\text{DM}} = 0.2$ with $M_t = 172.6 \text{ GeV}$ [see Figs. 4(e) and 4(g)], the LUX experiment has ruled out $m_S < 480 \text{ GeV}$. As a result, the MPCP is satisfied in the regions $5.5 \times 10^2 \text{ GeV} \leq m_S \leq 8.4 \times 10^2 \text{ GeV}$ and $6.3 \times 10^{13} \text{ GeV} \leq M_R \leq 1.6 \times 10^{14} \text{ GeV}$ for $\Omega_S/\Omega_{\text{DM}} = 0.5$ within $M_t = (172.6-174.1) \text{ GeV}$, and $m_S = 5.1 \times 10^2 \text{ GeV}$ and $M_R = 1.0 \times 10^{14} \text{ GeV}$ for $\Omega_S/\Omega_{\text{DM}} = 0.2$ with $M_t = 174.1 \text{ GeV}$. One can find that these m_S regions for the realization of the MPCP can also be consistent with the current DM direct detection experiments, and they will be checked by future DM direct searches.

Acknowledgement

This work is partially supported by Scientific Grant by the Ministry of Education and Science, No. 24540272. The work of R.T. is supported by research fellowships of the Japan Society for the Promotion of Science for Young Scientists.

References

- [1] G. Aad *et al.* [ATLAS Collaboration], Phys. Lett. B **716** (2012) 1 [arXiv:1207.7214 [hep-ex]].
- [2] S. Chatrchyan *et al.* [CMS Collaboration], JHEP **1306** (2013) 081 [arXiv:1303.4571 [hep-ex]].

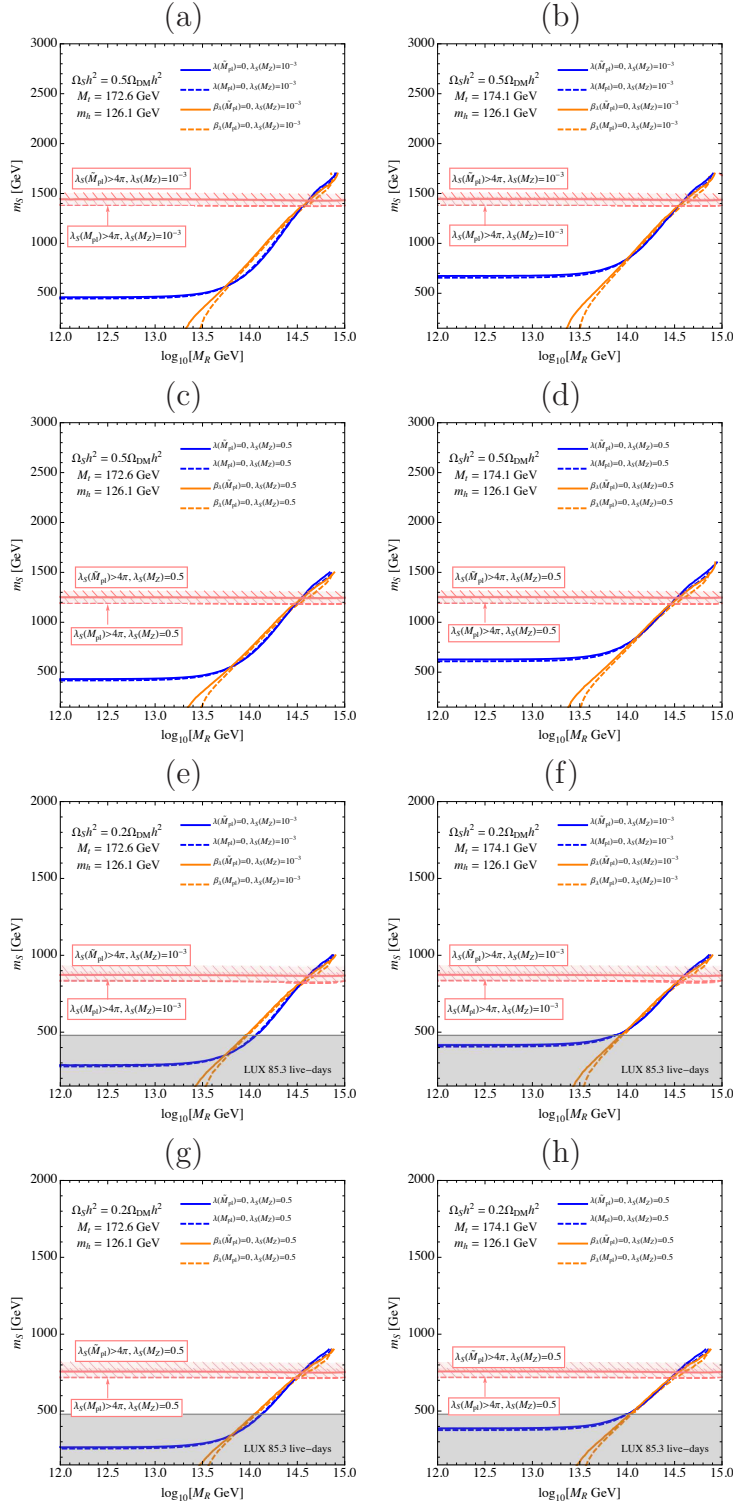


Figure 4: Numerical results for the realization of the MPCP [$\lambda = 0$ (blue curve) and $\beta_\lambda = 0$ (orange curve)] in the cases of $\Omega_S/\Omega_{\text{DM}} = 0.5$ [(a)-(d)] and $\Omega_S/\Omega_{\text{DM}} = 0.2$ [(e)-(h)]. The meanings of the figures are the same as in Fig. 1.

- [3] C. D. Froggatt and H. B. Nielsen, Phys. Lett. B **368** (1996) 96 [hep-ph/9511371].
- [4] M. Shaposhnikov and C. Wetterich, Phys. Lett. B **683** (2010) 196 [arXiv:0912.0208 [hep-th]].
- [5] M. Holthausen, K. S. Lim and M. Lindner, JHEP **1202** (2012) 037 [arXiv:1112.2415 [hep-ph]].
- [6] F. Bezrukov, M. Y. Kalmykov, B. A. Kniehl and M. Shaposhnikov, JHEP **1210** (2012) 140 [arXiv:1205.2893 [hep-ph]].
- [7] G. Degrassi, S. Di Vita, J. Elias-Miro, J. R. Espinosa, G. F. Giudice, G. Isidori and A. Strumia, JHEP **1208** (2012) 098 [arXiv:1205.6497 [hep-ph]].
- [8] S. Alekhin, A. Djouadi and S. Moch, Phys. Lett. B **716** (2012) 214 [arXiv:1207.0980 [hep-ph]].
- [9] I. Masina, Phys. Rev. D **87** (2013) 053001 [arXiv:1209.0393 [hep-ph]].
- [10] Y. Hamada, H. Kawai and K. -y. Oda, Phys. Rev. D **87** (2013) 053009 [arXiv:1210.2538 [hep-ph]].
- [11] F. Jegerlehner, arXiv:1304.7813 [hep-ph].
- [12] D. Buttazzo, G. Degrassi, P. P. Giardino, G. F. Giudice, F. Sala, A. Salvio and A. Strumia, JHEP **1312** (2013) 089 [arXiv:1307.3536].
- [13] I. Masina and M. Quiros, Phys. Rev. D **88** (2013) 093003 [arXiv:1308.1242 [hep-ph]].
- [14] A. Spencer-Smith, arXiv:1405.1975 [hep-ph].
- [15] V. Silveira and A. Zee, Phys. Lett. B **161** (1985) 136.
- [16] J. McDonald, Phys. Rev. D **50** (1994) 3637 [hep-ph/0702143 [hep-ph]].
- [17] C. P. Burgess, M. Pospelov and T. ter Veldhuis, Nucl. Phys. B **619** (2001) 709 [hep-ph/0011335].
- [18] H. Davoudiasl, R. Kitano, T. Li and H. Murayama, Phys. Lett. B **609** (2005) 117 [hep-ph/0405097].
- [19] B. Grzadkowski and J. Wudka, Phys. Rev. Lett. **103** (2009) 091802 [arXiv:0902.0628 [hep-ph]]; Acta Phys. Polon. B **40** (2009) 3007 [arXiv:0910.4829 [hep-ph]].
- [20] A. Drozd, B. Grzadkowski and J. Wudka, JHEP **1204** (2012) 006 [arXiv:1112.2582 [hep-ph]].

- [21] M. Kadastik, K. Kannike, A. Racioppi and M. Raidal, JHEP **1205** (2012) 061 [arXiv:1112.3647 [hep-ph]].
- [22] S. Baek, P. Ko and W. -I. Park, JHEP **1307** (2013) 013 [arXiv:1303.4280 [hep-ph]].
- [23] N. Haba, K. Kaneta, and R. Takahashi, arXiv:1309.1231 [hep-ph]; Eur. Phys. J. C **74** (2014) 2696 [arXiv:1309.3254 [hep-ph]].
- [24] N. Haba, K. Kaneta, and R. Takahashi, JHEP **1404** (2014) 029 [arXiv:1312.2089 [hep-ph]].
- [25] E. Gabrielli, M. Heikinheimo, K. Kannike, A. Racioppi, M. Raidal and C. Spethmann, Phys. Rev. D **89** (2014) 015017 [arXiv:1309.6632 [hep-ph]].
- [26] S. M. Boucenna, S. Morisi, Q. Shafi and J. W. F. Valle, arXiv:1404.3198 [hep-ph].
- [27] N. Haba and R. Takahashi, Phys. Rev. D **89** (2014) 115009 [arXiv:1404.4737 [hep-ph]].
- [28] Y. Hamada, H. Kawai and K. y. Oda, JHEP **1407** (2014) 026 [arXiv:1404.6141 [hep-ph]].
- [29] P. Ko and W. -I. Park, arXiv:1405.1635 [hep-ph].
- [30] N. Haba, H. Ishida and R. Takahashi, arXiv:1405.5738 [hep-ph].
- [31] P. A. R. Ade *et al.* [BICEP2 Collaboration], Phys. Rev. Lett. **112** (2014) 241101 [arXiv:1403.3985 [astro-ph.CO]].
- [32] F. L. Bezrukov and M. Shaposhnikov, Phys. Lett. B **659** (2008) 703 [arXiv:0710.3755 [hep-th]].
- [33] [ATLAS and CDF and CMS and D0 Collaborations], arXiv:1403.4427 [hep-ex].
- [34] P. A. R. Ade *et al.* [Planck Collaboration], arXiv:1303.5076 [astro-ph.CO].
- [35] G. Belanger, F. Boudjema, A. Pukhov and A. Semenov, Comput. Phys. Commun. **185** (2014) 960 [arXiv:1305.0237 [hep-ph]].
- [36] C. Faham [for the LUX Collaboration], arXiv:1405.5906 [hep-ex].
- [37] J. M. Cline, K. Kainulainen, P. Scott and C. Weniger, Phys. Rev. D **88** (2013) 055025 [arXiv:1306.4710 [hep-ph]].